

Antibody Profiling in COVID-19 Patients with Different Severities by Using Spike Variant Protein Microarrays

Wen-Yu Su,[▽] Pin-Xian Du,[▽] Harvey M. Santos,[▽] Tzong-Shiann Ho, Batuhan Birol Keskin, Chi Ho Pau, An-Ming Yang, Yi-Yu Chou, Hsi-Chang Shih, and Guan-Da Syu*



Cite This: *Anal. Chem.* 2022, 94, 6529–6539



Read Online

ACCESS |



Metrics & More

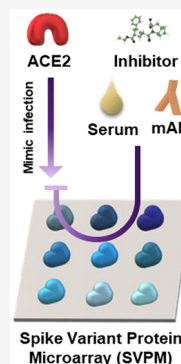


Article Recommendations



Supporting Information

ABSTRACT: The disease progression of COVID-19 varies from mild to severe, even death. However, the link between COVID-19 severities and humoral immune specificities is not clear. Here, we developed a multiplexed spike variant protein microarray (SVPM) and utilized it for quantifying neutralizing activity, drug screening, and profiling humoral immunity. First, we demonstrated the competition between antispike antibody and ACE2 on SVPM for measuring the neutralizing activity against multiple spike variants. Next, we collected the serums from healthy subjects and COVID-19 patients with different severities and profile the neutralizing activity as well as antibody isotypes. We identified the inhibition of ACE2 binding was stronger against multiple variants in severe compared to mild/moderate or critical patients. Moreover, the serum IgG against nonstructural protein 3 was elevated in severe but not in mild/moderate and critical cases. Finally, we evaluated two ACE2 inhibitors, Ramipril and Perindopril, and found the dose-dependent inhibition of ACE2 binding to all the spike variants except for B.1.617.3. Together, the SVPM and the assay procedures provide a tool for profiling neutralizing antibodies, antibody isotypes, and reagent specificities.



INTRODUCTION

The recently discovered coronavirus disease (COVID-19), induced by the novel severe acute respiratory syndrome coronavirus 2 (SARS-CoV-2), has put a burden on healthcare systems across the globe. The viral transmission has been accelerated not only by the incidence of asymptomatic outbreaks but also by the lack of broad screening and protective equipment for healthcare professionals worldwide.¹ The massive surge of COVID-19-infected patients into many hospitals necessitates a detailed understanding of the clinical, radiological, and laboratory findings linked to increased pathogenicity and fatality. The development of effective vaccines, on the other hand, has resulted in unprecedented confidence that the pandemic's end is near.² Unsurprisingly, the delayed vaccine rollout, the emergence of variants,³ combined with the lack of potent antiviral therapies, have left the world with the responsibility of managing the disease's uncertain nature. As a result, there is an immediate and continuous need to characterize the humoral antibody responses to this disease and its association with disease outcomes.

Patients infected with SARS-CoV-2 exhibit a wide variety of clinical symptoms ranging from mild infection to severe disease that can develop and lead to acute respiratory distress syndrome and, eventually, death.⁴ Nevertheless, while age⁵ and comorbidities have been associated with the progression of the disease,^{6,7} the course of SARS-CoV-2 infection remains uncertain. Since the first antibody tests were granted Emergency Use Authorization (EUA), most studies have focused on detecting SARS-CoV-2 specific immunoglobulin-M

(IgM) and immunoglobulin-G (IgG) antibodies mostly against one or two antigens: spike protein (S) and/or nucleoprotein (N),^{8–10} with far less investigating the immunoglobulin-A (IgA) antibody response in SARS-CoV-2 infected individuals.^{11,12} In addition to antibody isotypes, the neutralizing antibody represents the humoral defense against SARS-CoV-2 infections.^{13,14} Emerging immunological correlate analysis has revealed that initial strong neutralizing antibody responses,^{8,14} innate immune responses,¹⁵ and variable T cell and B cell populations¹⁶ and virus loads¹⁷ are all associated with different outcomes. Among such growing correlates, antibodies are linked to both the natural resolution of infection and the spread of disease.^{15,18} There is limited data on the extent and severity of symptoms in COVID-19 individuals and even less about the antibody profiles of the different disease severity (mild/moderate, severe, and critical). Therefore, a platform other than ELISA or lateral flow assays is needed to evaluate the complicated antibody specificity against multiple antigens from SARS-CoV-2 and their variants.

Protein microarray technologies can help address this gap, which could be used to aid in the development of vaccines or immunotherapies as treatment options.^{19,20} It is a great tool for studying the humoral immune responses, particularly the IgG,

Received: December 25, 2021

Accepted: April 11, 2022

Published: April 20, 2022



IgA, and IgM responses to SARS-CoV-2. Previously, we established a coronavirus array containing multiple antigens from various respiratory viruses and identified important markers for SARS-CoV-2 infections.¹² Other researchers also developed SARS-CoV-2 protein microarrays for profiling IgG and IgM responses in COVID-19 patients.^{20–22} However, the multiplexed platform for SARS-CoV-2 variants or for neutralizing assays is still missing. In the current study, we fabricated a multiplexed spike variant protein microarray (SVPM) containing spike proteins from different SARS-CoV-2 variants. By using the SVPM, we used a competition assay to evaluate the bindings of ACE2 to spike variants. Using this assay, we evaluated the efficacy of an antispike antibody, two ACE2 inhibitors, and profiled the serum antibodies in COVID-19 patients with different severities.

■ EXPERIMENTAL SECTION

Fabrication of Spike Variant Protein Microarrays (SVPMs). Fourteen blocks per slide were precoated with aldehyde and stored at 4 °C as previously described.¹² Each block on the slides was printed with 23 variant viral proteins including alpha/beta/gamma mutant type coronavirus, 5 cell lysates, and 8 control mix with 30% glycerol (Table S1) in technical triplicates to generate 9 × 12 formats by using a contact printer (CapitalBio SmartArrayer 136, China) at 4 °C. After printing, the SVPM was immobilized for 8 h, vacuum-sealed, and stored at –80 °C for future usage. The SVPM was stable at –80 °C for at least 6 months. The quality control of the SVPM was done by the fluorescence staining of his tagged proteins with 647-conjugated antihis (Jackson ImmunoResearch, no. 300-605-240) and showed 100% positive signals compared to the BSA and buffer control.

Competition between ACE2 and Antispike mAbs on SVPMs. The competition assay and the standard curve were described previously.²³ Briefly, the SVPMs stored at –80 °C were warmed to room temperature, added with 16-well cassettes, and then washed with TBST (TBS buffer with 0.1% Tween 20) for 10 min. The SVPMs were blocked with SuperBlock blocking buffer (ThermoFisher, no. 37515) for 15 min and incubated with serial dilutions of antispike antibody (Sino Biological, no. 40150-D001) for an hour. The arrays were washed with TBST and incubated with 50 μL of biotinylated human ACE2 125 pg/mL (Sino Biological, no. 10108-H08H-B), Cy5-conjugated streptavidin 2 ng/mL (Jackson ImmunoResearch, no. 016-170-084), and Cy3-conjugated antihuman IgG 1.5 μg/mL (Jackson ImmunoResearch, no. 109-165-003) for an hour. The arrays were washed, dried, and scanned for Cy3 and Cy5 signals with powers of 25% and 30% (Caduceus Biotechnology, #Spin-Scan).

Subjects and Ethical Statement. The protocol was reviewed according to the Declaration of Helsinki and approved by the Human Ethics Committee of National Cheng Kung University Medical College (IRB No.: A-ER-109-225). Serum samples were collected with the standard aseptic phlebotomy technique. The sera from healthy subjects were collected in 2019, before the COVID-19 pandemic. The sera from COVID-19 patients were collected without COVID-19 vaccination. The severity of the COVID-19 was classified based on the COVID-19 treatment guidelines panel, National Institutes of Health, United States (available at <https://www.covid19treatmentguidelines.nih.gov/>). Accessed 2022-03-02). Briefly, the subjects defined with mild/moderate COVID-19

were positive in PCR tests without admission to the hospital and shortness of breath, dyspnea, or abnormal chest imaging. The subjects defined with severe COVID-19 were positive in PCR tests with lowered oxygen saturations, with ventilators, and admission to the hospital but not in the intensive care unit. The subjects defined with critical COVID-19 were positive in PCR tests with lowered oxygen saturations, with ventilators, and admission to the intensive care unit. The COVID-19 serums were collected at least 5 days and a maximum of 60 days postsymptom onset. The sampling time after symptom onset for mild/moderate, severe, and critical COVID-19 were 31 ± 16 days, 27 ± 9 days, and 10 ± 11 days, respectively.

Profiling ACE2, IgG, IgA, and IgM Bindings in Serums. The SPVMs stored at –80 °C were warmed to room temperature, added with 16-well cassettes, and then washed with TBST for 10 min. Arrays were blocked with SuperBlock blocking buffer for 15 min and incubated with 50 μL of 50-fold diluted serum in TBST supplement with 1% BSA for an hour. After 1 h, the arrays were washed with TBST and incubated with 50 μL of biotinylated human ACE2 125 pg/mL, Cy5-conjugated streptavidin 2 ng/mL, and Cy3-labeled antihuman IgG/A/M antibodies (Jackson Laboratory, 75 ng/mL no. 109-165-008, 150 ng/mL no. 109-165-011, and 1.5 μg/mL no. 109-165-043) for an hour. The arrays were washed, dried, and scanned for Cy3 and Cy5 signals with power of 25% and 30%.

ACE2 Inhibitor Binding Assay. Two ACE2 inhibitors, Ramipril and Perindopril,²⁴ were dissolved in PBS (Sigma-Aldrich, no. R0404, no. P0094). The SPVMs stored at –80 °C were warmed to room temperature, added with 16-well cassettes, washed with TBST for 10 min, and blocked by SuperBlock for 15 min. The biotinylated ACE2 125 pg/mL was preincubated with serial dilutions of inhibitors in PBS for 10 min and then added to the blocked SVPMs for an hour. After 1 h, the arrays were washed with TBST and incubated with 50 μL of Cy5-conjugated streptavidin 2 ng/mL for another hour. The arrays were then washed, dried, and scanned for Cy3 and Cy5 signals with power of 25% and 30%.

Data Analysis. The fluorescence signals were analyzed by GenePix Pro software as foreground minus background. ACE2 binding was defined by the percentage of ACE2 fluorescence intensity with sample divided by ACE2 fluorescence intensity without sample. For IgG/A/M profiling, the signals from viral proteins were divided by their antihis signals to normalize the protein amounts. A few outliers were identified and removed by Grubbs' method with alpha 0.0001. One-way ANOVA with Tukey's multiple comparisons and two-way ANOVA with Dunnett's multiple comparisons were used to compare multiple groups. For the baseline characteristics, data were analyzed by Mann–Whitney tests for continuous variables or by Chi-square tests for categorical variables. Data were calculated by GraphPad Prism 8 where $p < 0.05$ was the threshold for significance. All data and figures were presented as mean ± SD.

■ RESULTS AND DISCUSSION

Design and Fabrication of Spike Variant Protein Microarray (SVPM). To profile the antibody responses in COVID-19, our team and others have previously focused on the antigens from wild-type SARS-CoV-2 and built SARS-CoV-2 protein microarrays or bead arrays.^{10,12,20–22} However, the SARS-CoV-2 has mutated through time, leading to widespread viral variants with different transmission efficiency, fatality, and resistance to antibody neutralization.²⁵ Hence, our

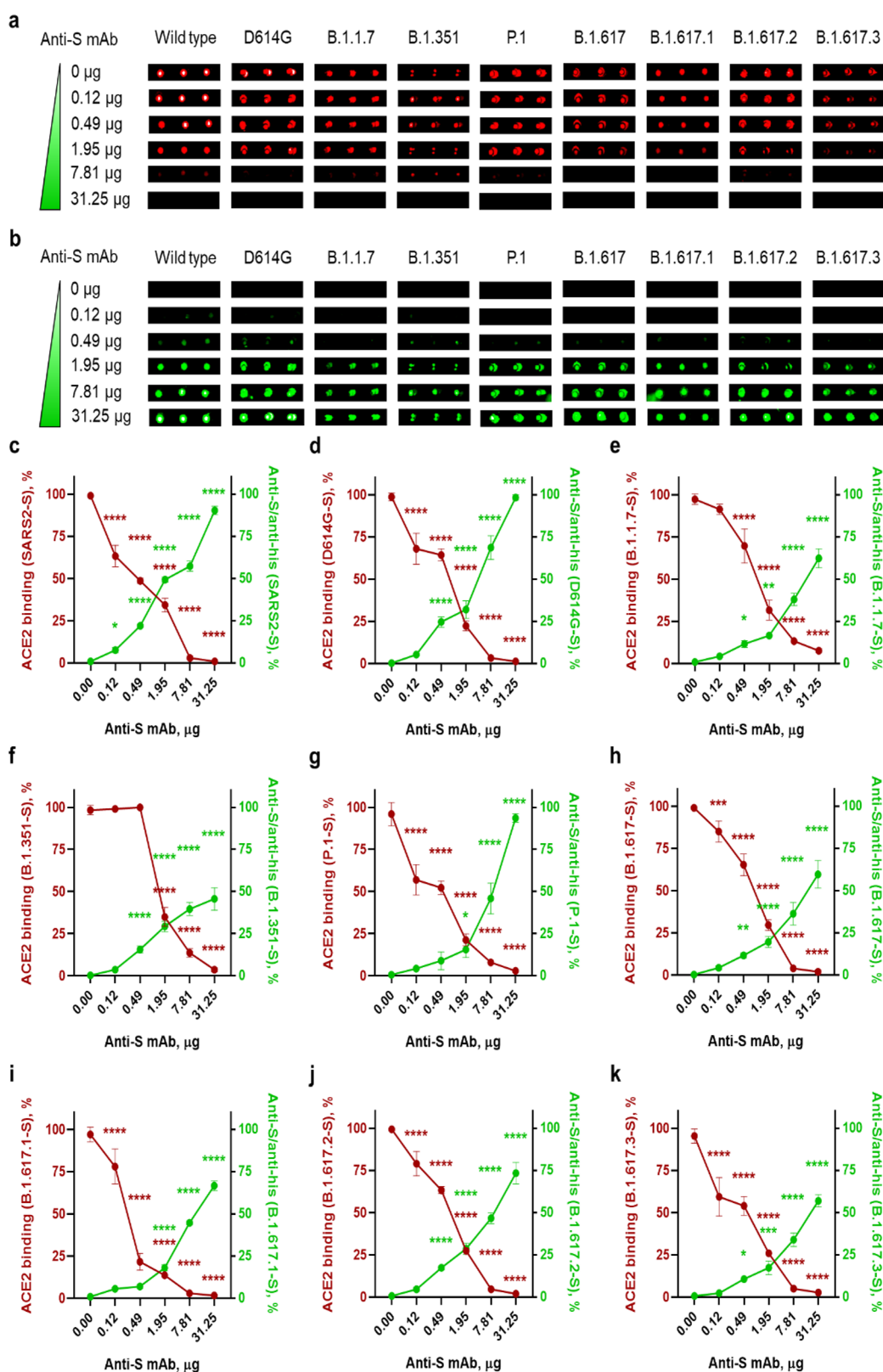


Figure 1. Profiling the neutralizing activity for antispike mAb by using an *in vitro* spike variant protein microarray (SVPM). SVPM was first incubated with antispike mAb and then incubated with Cy3-labeled antihuman antibody and Cy5-labeled ACE2 to mimic the attachment of viruses. (a) Images of ACE2 bound to spike variants in the presence or absence of antispike mAb. (b) Images of antispike bound to spike variants in a dose-dependent manner. (c–k) Dual quantification of the ACE2 and antispike bindings against spike proteins from SARS-CoV-2 wildtype and variants, including D614G, B.1.1.7, B.1.351, P.1, B.1.617, B.1.617.1, B.1.617.2, and B.1.617.3. The ACE2 binding was normalized by the antibody-free group for indicating the full attachment of viruses. Data were analyzed by two-way ANOVA with Dunnett's multiple comparisons. * $p < 0.05$, ** $p < 0.01$, *** $p < 0.005$, and **** $p < 0.001$ compared with the zero dose of anti-S.

Table 1. Baseline Characteristics of Healthy and COVID-19 Subjects^a

classifications	healthy (H)	mild/moderate (M)	severe (S)	critical (C)	M vs C <i>p</i> value	S vs C <i>p</i> value	M vs S <i>p</i> value
age (years, SD)	69 (9)	45 (15)	56 (17)	72 (11)	<0.0001	0.0002	0.0237
gender (male, %)	12 (46%)	13 (52%)	13 (57%)	16 (53%)	0.9214	0.8172	0.7534
deceased (<i>N</i> , %)	0 (0%)	0 (0%)	0 (0%)	12 (40%)	0.0003	0.0006	1.0000
diabetes (<i>N</i> , %)	0 (0%)	2 (8%)	3 (13%)	15 (50%)	0.0008	0.0049	0.5677
hypertension (<i>N</i> , %)	0 (0%)	3 (12%)	8 (35%)	9 (30%)	0.1075	0.7116	0.0606
cardiovascular disease (<i>N</i> , %)	0 (0%)	0 (0%)	2 (9%)	4 (13%)	0.058	0.5974	0.132

^aData were shown as means (SD) and analyzed by Mann–Whitney tests or shown as counts (%) and analyzed by Chi-square tests.

current work is to build a high-throughput platform for the detection, prevention, and therapeutic interventions of COVID-19 infected people with SARS-CoV-2 variants.

The spike variant protein microarray (SVPM) was fabricated containing 23 viral antigens including the spike proteins, nonstructural proteins, nucleocapsid proteins, 5 cell membranes, and 8 controls. The viral antigens printed and immobilized on this protein microarray were from epidemic coronaviruses which included SARS-CoV-2, SARS-CoV, MERS-CoV, common cold coronaviruses (HKU1-CoV, 229E-CoV, and NL63-CoV), and the eight common SARS-CoV-2 variants. The complete list of the proteins and control samples that were used in this study is presented in Table S1. The viral antigens and control samples were then spotted on the aldehyde slides in triplicate with 14 identical blocks and formed a multiplexed SVPM (Figure S1).

Dual Profiling of ACE2 and Antispike Bindings with the SVPM. A neutralizing antibody (NAb) is an antibody that is responsible for blocking infections. In COVID-19, NABs are generally referred to antispike antibodies which can prevent the bindings to the host ACE2 receptors.^{23,26} Three steps were used to confirm the protein function on the arrays and establish the neutralizing assays *in vitro*. First, we confirmed the binding of ACE2 to the wild-type and eight spike variants on the SVPM (Figure 1A, first row). Given that the viral antigens in the SVPM were functional, we aimed to quantify both antispike and ACE2 bindings by using two independent fluorescence signals. Next, we utilized a humanized antispike monoclonal antibody (mAb) as a proof of concept to detect the specificity of antibody affinities. We established the dose-dependent bindings of antispike mAb to the wild-type and eight spike variants on the SVPM (Figure 1b–k). Finally, we demonstrated the competition between antispike mAb and ACE2 to the wild-type and eight spike variants on the SVPM (Figure 1a,c–k). The antispike mAb that we tested here showed broad NAb capabilities against wild-type and eight common SARS-CoV-2 variants.

Profiling the ACE2 Binding in Subjects with Different COVID-19 Severities. To investigate the antibody responses in subjects with different COVID-19 severities, we collected sera from mild/moderate (M), severe (S), and critical (C) as well as healthy (H) subjects. The average data for blood sampling after symptom onset was 31 ± 16 days for the M group, 27 ± 9 days for the S group, and 10 ± 11 days for the C group. The sampling time for the C group was earlier than other groups due to the multiple organ failure. It is worth noting that the sampling time was not correlated with any antibody data observed in this study. The baseline characteristics, including age, gender, deceased, diabetes, hypertension, and cardiovascular disease, were listed and analyzed in Table 1. For the detailed clinical data, please see the Supporting Information. Among those baseline characteristics, age,

deceased, and diabetes were significant factors in the critical cases (Table 1). Our findings align with other clinical meta-analyses.²⁷

Considering SARS-CoV-2 relies predominantly on ACE2 for fusion and entry, distinct genetic variants of spike proteins may change binding interactions and susceptibility to the disease.²⁸ Thus, we investigated the bindings of ACE2 in wild-type and eight spike variants in patients with different COVID-19 severities (Figure 2 and Figure S2). The SVPMs were first incubated with sera for an hour, washed, incubated with Cy3-labeled antihuman and Cy5-labeled ACE2 for another hour, washed, dried, and scanned for the fluorescent images (Figure 2a and Figure S1). All the COVID-19 subjects showed significant inhibition of the ACE2 bindings compared to the H group (Figure 2b–j). Compared with the M group, the S group showed more inhibition of the ACE2 bindings in wild-type, B.1.1.7, P.1, and B.1.617 (Figure 2b,d,f,g). Compared with the C group, the S group showed more inhibition of the ACE2 bindings in D614G, B.1.351, P.1, B.1.617, B.1.617.1, B.1.617.2, and B.1.617.3 (Figure 2c,e–j). The detailed ACE2 data were listed in the Supporting Information. ACE2 binding is a good marker to distinguish healthy from COVID-19 patients. The increment of neutralizing antibody against wild-type SARS-CoV-2 has been linked with clinical severities.¹⁵ Here, we demonstrated a broad spectrum of neutralizing antibodies against multiple variants in the COVID-19 patients and more enhanced in the severe cases. It could be the key that COVID-19 patients with severe symptoms did not undergo critical symptoms.

Profiling the IgG in Subjects with Different COVID-19 Severities. To better understand the humoral immune responses against SARS-CoV-2 and its variants as well as COVID-19 severities, we profiled the antibody isotypes in COVID-19 patients with different severities. Except for immunocompromised patients, the production of specific antibodies against SARS-CoV-2 is consistent during infection. One of which is the high-affinity IgG responses that are essential for long-term immunological memory.¹² Since the SVPM utilized structural proteins, e.g., spike (S) and nucleocapsid (N), and nonstructural proteins, e.g., the largest nonstructural protein (NSP3) and RNA-dependent RNA polymerase (RdRp), it is essential to evaluate the IgG responses based on these viral antigens.

The IgG against wild-type and eight spike variants were quantified and visualized in a heatmap format (Figure S3). IgG against spikes was generally higher in COVID-19 patients but not in the S group (Figure 3). Lower IgG levels against B.1.1.7-S, B.1.351-S, P.1-S, B.1.617-S, B.1.617.1-S, B.1.617.2-S, and B.1.617.3-S were found in the S group compared to the M group (Figure 3c–i). The IgG against NSP3 was only increased in the S group, which could be a marker to separate the H, M, and C groups (Figure 3k). The detailed IgG data

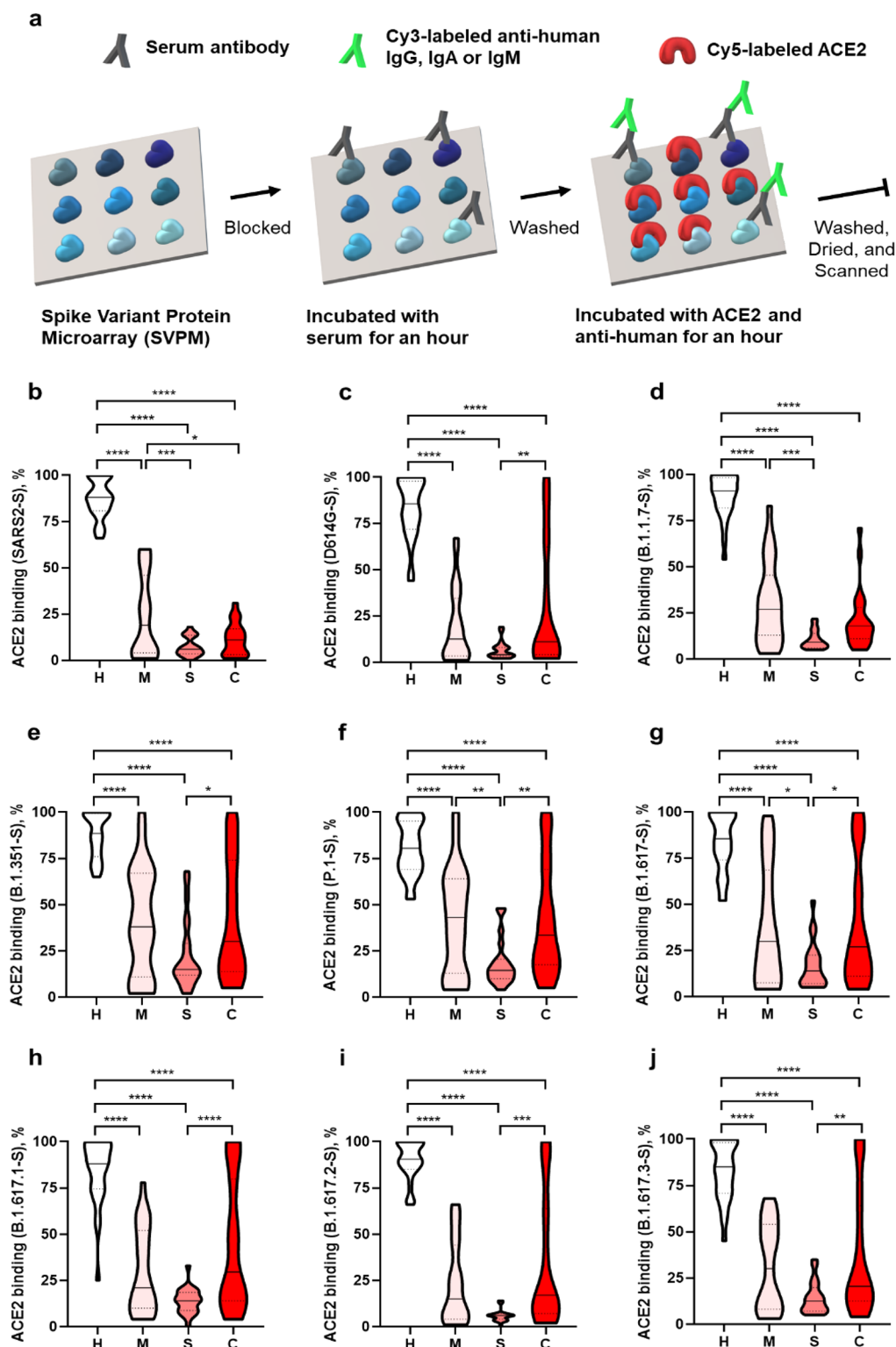


Figure 2. Profiling the neutralizing activity in healthy control (H), mild/moderate (M), severe (S), and critical (C) subjects by using SVPM. (a) SVPM was first incubated with serums for an hour, washed, incubated with Cy3-labeled antihuman IgG/A/M and Cy5-labeled ACE2 for an hour, washed, dried, and scanned for the fluorescent image. (b–j) Serums from healthy COVID-19 subjects were used to quantify the ACE2 bindings against various spike proteins by using SVPM. The ACE2 bindings were normalized by the serum-free group. Data were analyzed by one-way ANOVA with Tukey's multiple comparisons. * $p < 0.05$, ** $p < 0.01$, *** $p < 0.005$, and **** $p < 0.001$ compared with indicated groups. The number of subjects in the H, M, S, and C groups was 26, 25, 23, and 30, respectively.

were listed in the [Supporting Information](#). The high level of IgG against NSP3 may indicate broad viral replication in the host cells and elevate the antigen presentation of this largest nonstructural protein, NSP3. Recently, NSP3 has been

investigated as a potential antibody biomarker of severe COVID-19 patients.²⁹ IgG against other nonstructural proteins has also been reported in severe COVID-19 cases.²¹ Although it is unknown why antibodies against NSPs are related to

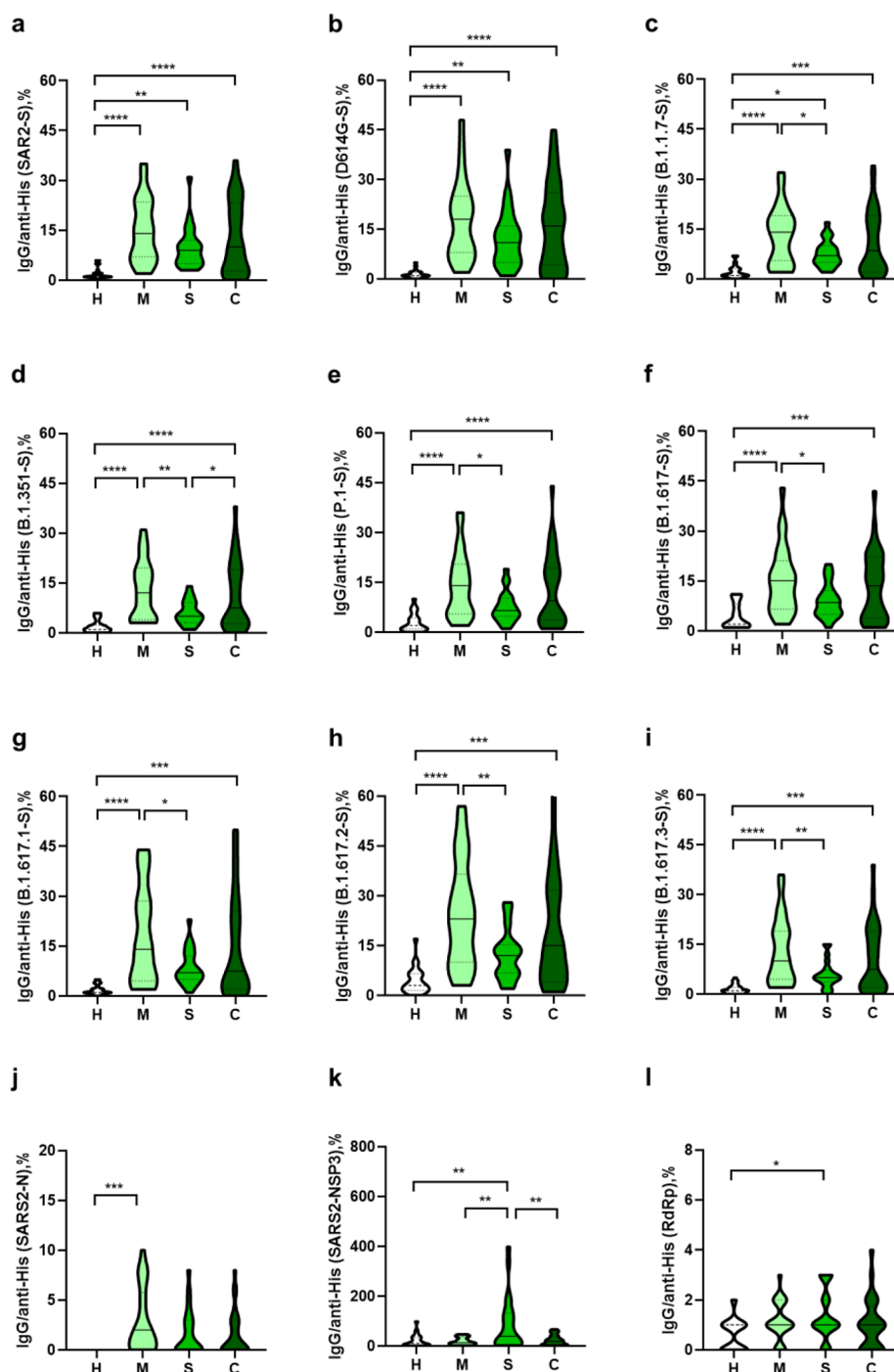


Figure 3. Profiling the serum IgG in healthy control (H), mild/moderate (M), severe (S), and critical (C) subjects by using SVPM. (a–i) Serums from healthy and COVID-19 subjects were used to quantify the IgG bindings against various spike proteins by using SVPM. (j–l) Serum IgG bindings to the structural and nonstructural proteins from SARS-CoV-2. Data were analyzed by one-way ANOVA with Tukey’s multiple comparisons. * $p < 0.05$, ** $p < 0.01$, *** $p < 0.005$, and **** $p < 0.001$ compared with indicated groups. The number of subjects in the H, M, S, and C groups was 26, 25, 23, and 30, respectively.

severe COVID-19, NSPs are implicated in key functions including viral infection, including SARS-CoV-2 RNA preservation, replication, transcription, polyprotein assembly, and host innate immune inactivation.

Profiling the IgA in Subjects with Different COVID-19 Severities. The human receptor ACE2, which is produced by alveolar epithelial cells, allows the virus to hijack and enter host cells. Conversely, switching between antibody classes can result in the production of IgA. Plasma cells in the lamina propria

close to mucosal membranes produce the majority of IgA.³⁰ This isotype switching does not alter the antibody’s specificity but rather allows for various biological effects via the antibody’s tail region.

A systematic investigation of IgA production in COVID-19 patients is lacking, thus we further investigated the IgA responses in COVID-19 patients at different levels of severity (Figure 4 and Figure S4). Interestingly, in the SARS-CoV-2 variants, IgA can effectively separate COVID-19 patients

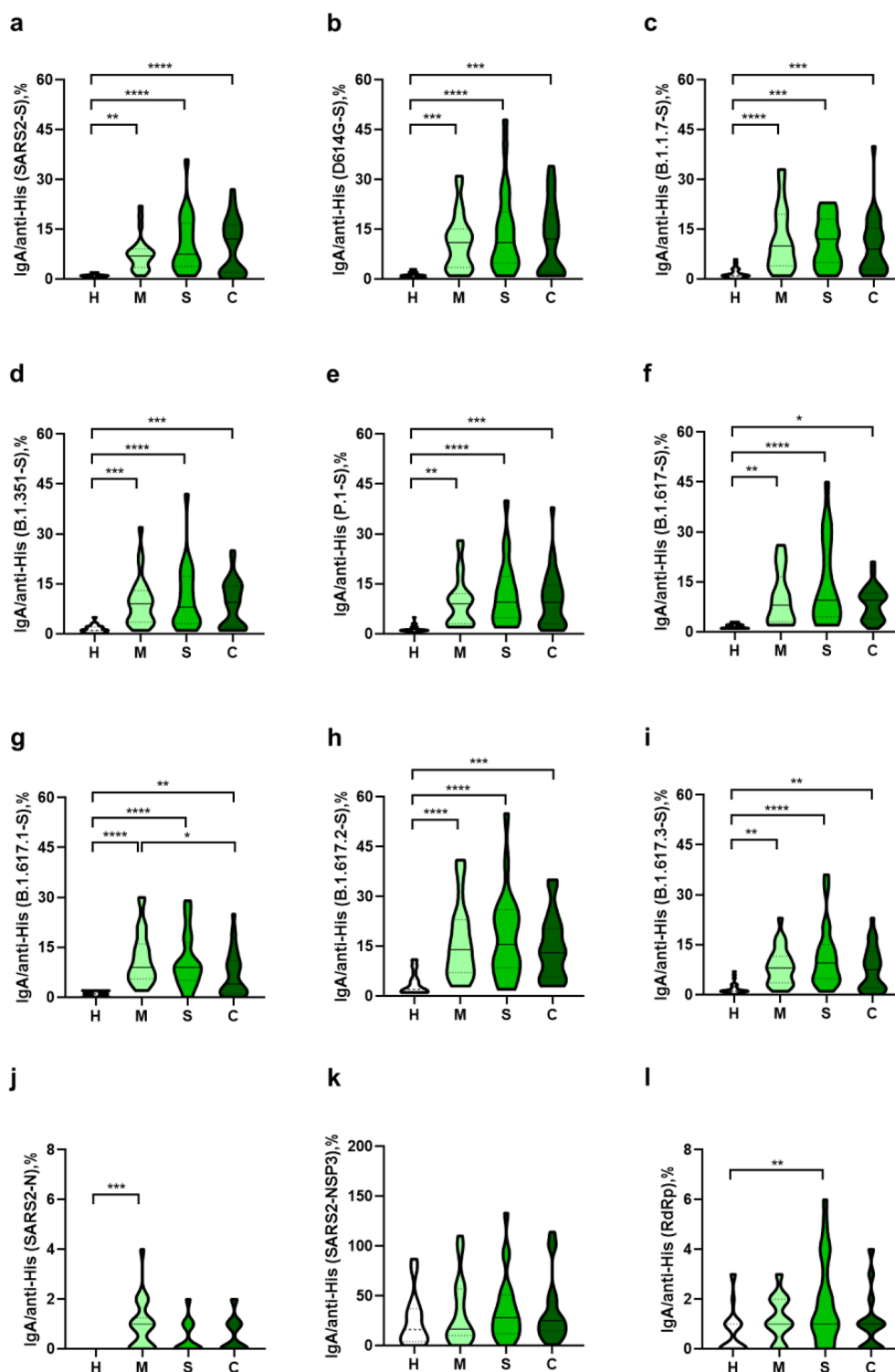


Figure 4. Profiling the serum IgA in healthy control (H), mild/moderate (M), severe (S), and critical (C) subjects by using SVPM. (a–i) Serums from healthy COVID-19 subjects were used to quantify the IgA bindings against various spike proteins by using SVPM. (j–l) Serum IgA bindings to the structural and nonstructural proteins from SARS-CoV-2. Data were analyzed by one-way ANOVA with Tukey’s multiple comparisons. * $p < 0.05$, ** $p < 0.01$, *** $p < 0.005$, and **** $p < 0.001$ compared with the indicated groups. The number of subjects in the H, M, S, and C groups was 26, 25, 23, and 30, respectively.

(Figure 4a–i). However, in B.1.617 variants, the IgA was lower in the C group but higher in the M group (Figure 4g). The detailed IgA data are listed in the Supporting Information. Although IgA is crucial for mucosal immunity, it is the most critical immunoglobulin for fighting infectious pathogens in the

respiratory and digestive systems at the point of pathogen invasion. Secretory IgA, as an immunological barrier, can neutralize SARS-CoV-2 before it reaches and binds to epithelial cells.^{6,30} In addition, IgA and IgG against N protein were only higher in the M group which could be a marker to

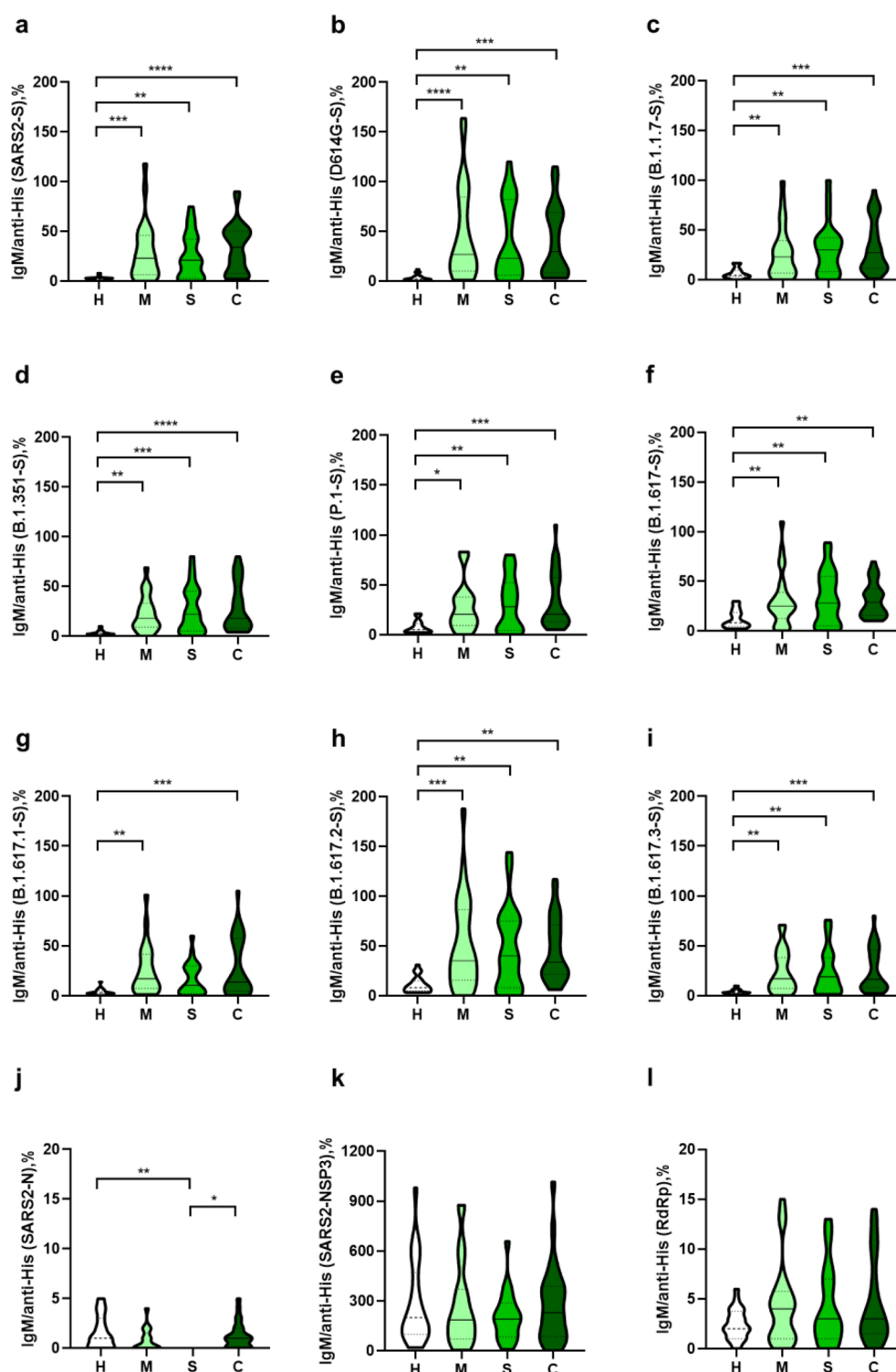


Figure 5. Profiling the serum IgM in healthy control (H), mild/moderate (M), severe (S), and critical (C) subjects by using SVPM. (a–i) Serums from healthy and COVID-19 subjects were used to quantify the IgM bindings against various spike proteins by using SVPM. (j–l) Serum IgM bindings to the structural and nonstructural proteins from SARS-CoV-2. Data were analyzed by one-way ANOVA with Tukey's multiple comparisons. * $p < 0.05$, ** $p < 0.01$, *** $p < 0.005$, and **** $p < 0.001$ compared with indicated groups. The number of subjects in the H, M, S, and C groups was 26, 25, 23, and 30, respectively.

separate severe and critical patients (Figures 3j and 4j). This could indicate a better diversity of structural protein presentation rather than focusing on presenting the S protein. IgA and IgG against RdRp were only higher in the S group (Figures 3l and 4l). It is a good marker for severe COVID-19

and could be an indication that the SARS-CoV-2 is infecting a lot of host cells.

Profiling the IgM in Subjects with Different COVID-19 Severities. Rapid and specific IgM and IgG antibody testing in suspected SARS-CoV-2 individuals could provide informa-

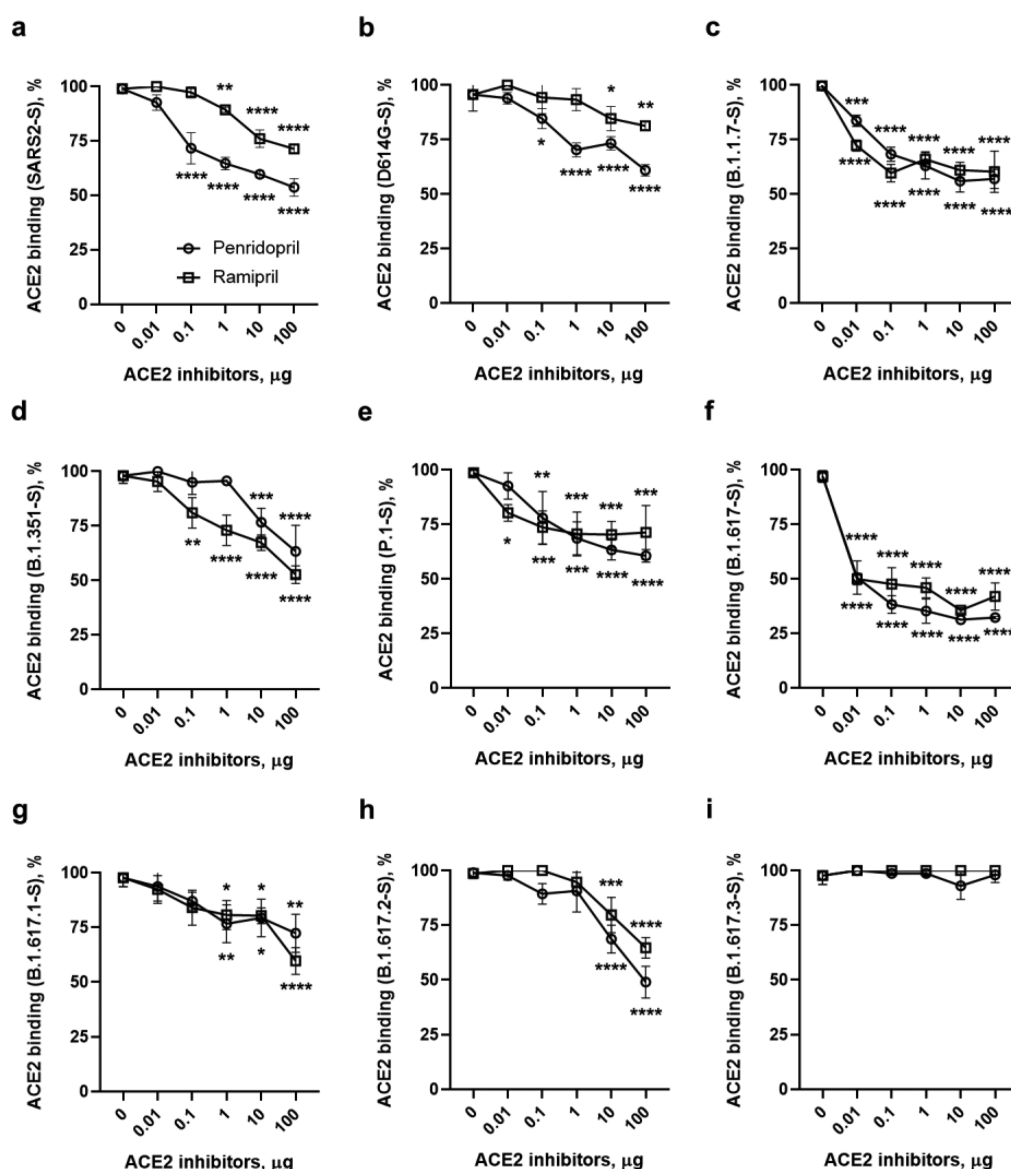


Figure 6. Profiling the neutralizing activity for ACE2 inhibitors by using SVPM. (a–i) Two ACE2 inhibitors, e.g., Penridopril and Ramipril, were used to profile the binding of ACE2 against multiple spike variants by using SVPM. The ACE2 binding was normalized by the inhibitor-free group for indicating the full attachment of viruses. Data were analyzed by two-way ANOVA with Dunnett's multiple comparisons. * $p < 0.05$, ** $p < 0.01$, *** $p < 0.005$, and **** $p < 0.001$ compared with the zero dose of anti-S.

tion for validation or exclusion of SARS-CoV-2 infection. The IgM against wild-type and eight spike variants were quantified and visualized in a heatmap format (Figure S5). In our study, the IgM can effectively separate the COVID-19 patients (Figure 5a–i). The detailed IgM data were listed in the Supporting Information. This COVID-19 study has some limitations, and we do not have the patient data of which variant they were infected. However, based on the sampling time, the dominant variant was B.1.1.7. In this study, we only presented the humoral immunity of COVID-19 patients with different levels of severities which do not fully represent the whole immunity against SARS-CoV-2.

Profiling the Neutralizing Activity for ACE2 inhibitors by using SVPM. To provide the specificity of potential treatments, we select two ACE2 inhibitors, e.g., Ramipril and Penridopril.²⁴ Both inhibitors can dose-dependently decrease the ACE2 bindings to the spike proteins, except for the B.1.617.3 variant (Figure 6). Compared with the antispike

mAb, the inhibitors showed much lower potency in blocking the ACE2 and spike interactions (Figure 1).

CONCLUSION

In this work, we fabricated a multiplexed spike variant protein microarray (SVPM) that enables the detection of neutralizing antibodies and antibody isotypes against wild-type and SARS-CoV-2 variants in a high-throughput manner. We utilized the SVPM platform to profile an antibody drug, small molecule inhibitors, and serum antibodies in COVID-19 patients with different severities.

ASSOCIATED CONTENT

Supporting Information

The Supporting Information is available free of charge at <https://pubs.acs.org/doi/10.1021/acs.analchem.1c05567>.

Additional experimental details, materials, and figures (PDF)

Detailed clinical data and raw microarray data (XLSX)

AUTHOR INFORMATION

Corresponding Author

Guan-Da Syu – Department of Biotechnology and Bioindustry Sciences and Research Center of Excellence in Regenerative Medicine, National Cheng Kung University, Tainan 701, Taiwan; Medical Device Innovation Center, National Cheng Kung University, Tainan 701, Taiwan; orcid.org/0000-0003-4661-414X; Phone: +886-6-275-7575 #58231; Email: guanda@gs.ncku.edu.tw; Fax: +886-6-276-6490

Authors

Wen-Yu Su – Department of Biotechnology and Bioindustry Sciences, National Cheng Kung University, Tainan 701, Taiwan

Pin-Xian Du – Department of Biotechnology and Bioindustry Sciences, National Cheng Kung University, Tainan 701, Taiwan

Harvey M. Santos – Department of Biotechnology and Bioindustry Sciences, National Cheng Kung University, Tainan 701, Taiwan; School of Chemical, Biological and Materials Engineering and Sciences, Mapúa University, Manila 1002, Philippines; orcid.org/0000-0002-6514-9565

Tzong-Shiann Ho – Department of Pediatrics, National Cheng Kung University Hospital, College of Medicine, National Cheng Kung University, Tainan 701, Taiwan; Center of Infectious Disease and Signaling Research, National Cheng Kung University, Tainan 701, Taiwan; Department of Pediatrics, Tainan Hospital, Ministry of Health and Welfare, Tainan 700, Taiwan

Batuhan Birol Keskin – Department of Biotechnology and Bioindustry Sciences, National Cheng Kung University, Tainan 701, Taiwan

Chi Ho Pau – Department of Biotechnology and Bioindustry Sciences, National Cheng Kung University, Tainan 701, Taiwan

An-Ming Yang – Department of Internal Medicine, En Chu Kong Hospital, New Taipei City 237, Taiwan; Department of Nursing, Yuanpei University of Medical Technology, Hsinchu 300, Taiwan

Yi-Yu Chou – Department of Nursing, Kaohsiung Armed Forces General Hospital, Kaohsiung 802, Taiwan

Hsi-Chang Shih – Department of Pharmacology and Molecular Sciences, Johns Hopkins University School of Medicine, Baltimore, Maryland 21205, United States

Complete contact information is available at:

<https://pubs.acs.org/10.1021/acs.analchem.1c05567>

Author Contributions

W.-Y.S., P.-X.D., and H.M.S. are co-first authors. W.-Y.S., P.-X.D., H.M.S., G.-D.S., T.-S.H., Y.-Y.C., B.B.K., C.H.P., A.-M.Y., and H.-C.S. performed the experimental work. G.-D.S., H.M.S., P.-X.D., and W.-Y.S. contributed to the manuscript preparation. G.-D.S. contributed their expertise and supervision to the entire project.

Notes

The authors declare no competing financial interest.

ACKNOWLEDGMENTS

This work was supported in part by the Ministry of Science and Technology, Grants MOST-110-2628-B-006-022- (G.-D.S.), MOST-108-2320-B-006-054-MY2 (G.-D.S.), MOST 110-2731-M-006-001 (G.-D.S.), MOST-109-2327-B-006-005- (G.-D.S., T.-S.H.), MOST 111-2321-B-006-009- (T.-S.H.), MOST-110-2622-E-006-030 (T.-S.H.), MOST-110-2327-B-006-005 (T.-S.H.), NHRI-110A1-MRCO-02212103 (T.-S.H.), NCKUH-11002018 (T.-S.H.), Medical Research Fund of Kaohsiung Armed Forces General Hospital KAFGH-D-108024 (Y.-Y.C.), KAFGH-D-109042 (Y.-Y.C.), KAFGH-D-110035 (Y.-Y.C.), KAFGH-D-111033 (Y.-Y.C.), and Headquarters of University Advancement at the National Cheng Kung University, Ministry of Education, Taiwan. We thank Prof. Chien-Sheng Chen for providing the microarray printer and NHRI Biobank for providing specimens.

REFERENCES

- (1) Gondi, S.; Beckman, A. L.; Deveau, N.; Raja, A. S.; Ranney, M. L.; Popkin, R.; He, S. *Lancet* **2020**, 395 (10237), e90–e91.
- (2) Polack, F. P.; Thomas, S. J.; Kitchin, N.; Absalon, J.; Gurtman, A.; Lockhart, S.; Perez, J. L.; Perez Marc, G.; Moreira, E. D.; Zerbini, C.; Bailey, R.; Swanson, K. A.; Roychoudhury, S.; Koury, K.; Li, P.; Kalina, W. V.; Cooper, D.; Frenck, R. W.; Hammitt, L. L.; Tureci, O.; Nell, H.; Schaefer, A.; Unal, S.; Tresnan, D. B.; Mather, S.; Dormitzer, P. R.; Sahin, U.; Jansen, K. U.; Gruber, W. C. *N. Engl. J. Med.* **2020**, 383, 2603–2615.
- (3) Chen, R. E.; Zhang, X.; Case, J. B.; Winkler, E. S.; Liu, Y.; VanBlargan, L. A.; Liu, J.; Errico, J. M.; Xie, X.; Suryadevara, N.; Gilchuk, P.; Zost, S. J.; Tahan, S.; Droit, L.; Turner, J. S.; Kim, W.; Schmitz, A. J.; Thapa, M.; Wang, D.; Boon, A. C. M.; Presti, R. M.; O'Halloran, J. A.; Kim, A. H. J.; Deepak, P.; Pinto, D.; Fremont, D. H.; Crowe, J. E.; Corti, D.; Virgin, H. W.; Ellebedy, A. H.; Shi, P.-Y.; Diamond, M. S. *Nat. Med.* **2021**, 27 (4), 717–726.
- (4) Gupta, A.; Madhavan, M. V.; Sehgal, K.; Nair, N.; Mahajan, S.; Sehrawat, T. S.; Bikdeli, B.; Ahluwalia, N.; Ausiello, J. C.; Wan, E. Y.; Freedberg, D. E.; Kirtane, A. J.; Parikh, S. A.; Maurer, M. S.; Nordvig, A. S.; Accili, D.; Bathon, J. M.; Mohan, S.; Bauer, K. A.; Leon, M. B.; Krumholz, H. M.; Uriel, N.; Mehra, M. R.; Elkind, M. S. V.; Stone, G. W.; Schwartz, A.; Ho, D. D.; Bilezikian, J. P.; Landry, D. W. *Nat. Med.* **2020**, 26 (7), 1017–1032.
- (5) Liu, K.; Chen, Y.; Lin, R.; Han, K. *Journal of Infection* **2020**, 80 (6), e14–e18.
- (6) Suthar, M. S.; Zimmerman, M. G.; Kauffman, R. C.; Mantus, G.; Linderman, S. L.; Hudson, W. H.; Vanderheiden, A.; Nyhoff, L.; Davis, C. W.; Adekunle, O.; Affer, M.; Sherman, M.; Reynolds, S.; Verkerke, H. P.; Alter, D. N.; Guarner, J.; Bryksin, J.; Horwath, M. C.; Arthur, C. M.; Saakadze, N.; Smith, G. H.; Edupuganti, S.; Scherer, E. M.; Hellmeister, K.; Cheng, A.; Morales, J. A.; Neish, A. S.; Stowell, S. R.; Frank, F.; Ortlund, E.; Anderson, E. J.; Menachery, V. D.; Rouphael, N.; Mehta, A. K.; Stephens, D. S.; Ahmed, R.; Roback, J. D.; Wrappert, J. *Cell Reports Medicine* **2020**, 1 (3), 100040.
- (7) Zhou, F.; Yu, T.; Du, R.; Fan, G.; Liu, Y.; Liu, Z.; Xiang, J.; Wang, Y.; Song, B.; Gu, X.; Guan, L.; Wei, Y.; Li, H.; Wu, X.; Xu, J.; Tu, S.; Zhang, Y.; Chen, H.; Cao, B. *Lancet* **2020**, 395 (10229), 1054–1062.
- (8) Long, Q.-X.; Liu, B.-Z.; Deng, H.-J.; Wu, G.-C.; Deng, K.; Chen, Y.-K.; Liao, P.; Qiu, J.-F.; Lin, Y.; Cai, X.-F.; Wang, D.-Q.; Hu, Y.; Ren, J.-H.; Tang, N.; Xu, Y.-Y.; Yu, L.-H.; Mo, Z.; Gong, F.; Zhang, X.-L.; Tian, W.-G.; Hu, L.; Zhang, X.-X.; Xiang, J.-L.; Du, H.-X.; Liu, H.-W.; Lang, C.-H.; Luo, X.-H.; Wu, S.-B.; Cui, X.-P.; Zhou, Z.; Zhu, M.-M.; Wang, J.; Xue, C.-J.; Li, X.-F.; Wang, L.; Li, Z.-J.; Wang, K.; Niu, C.-C.; Yang, Q.-J.; Tang, X.-J.; Zhang, Y.; Liu, X.-M.; Li, J.-J.; Zhang, D.-C.; Zhang, F.; Liu, P.; Yuan, J.; Li, Q.; Hu, J.-L.; Chen, J.; Huang, A.-L. *Nat. Med.* **2020**, 26 (6), 845–848.
- (9) Clapham, H.; Hay, J.; Routledge, I.; Takahashi, S.; Choisy, M.; Cummings, D.; Grenfell, B.; Metcalf, C. J. E.; Mina, M.; Barraquer, I.

- R.; Salje, H.; Tam, C. C. *Emerg. Infect. Dis.* **2020**, *26* (9), 1978. Okba, N. M. A.; Müller, M. A.; Li, W.; Wang, C.; GeurtsvanKessel, C. H.; Corman, V. M.; Lamers, M. M.; Sikkema, R. S.; de Bruin, E.; Chandler, F. D.; et al. *Emerg Infect Dis* **2020**, *26* (7), 1478–1488.
- (10) Roxhed, N.; Bendes, A.; Dale, M.; Mattsson, C.; Hanke, L.; Dodig-Crnković, T.; Christian, M.; Meineke, B.; Elsässer, S.; Andréll, J.; et al. *Nat. Commun.* **2021**, *12* (1), 3695.
- (11) Behrens, G. M.; Cossmann, A.; Stankov, M. V.; Witte, T.; Ernst, D.; Happle, C.; Jablonka, A. *Infection* **2020**, *48* (4), 631–634.
- (12) Du, P.-X.; Chou, Y.-Y.; Santos, H. M.; Keskin, B. B.; Hsieh, M.-H.; Ho, T.-S.; Wang, J.-Y.; Lin, Y.-L.; Syu, G.-D. *Anal. Chem.* **2021**, *93*, 7690.
- (13) Khoury, D. S.; Cromer, D.; Reynaldi, A.; Schlub, T. E.; Wheatley, A. K.; Juno, J. A.; Subbarao, K.; Kent, S. J.; Triccas, J. A.; Davenport, M. P. *Nat. Med.* **2021**, *27* (7), 1205–1211.
- (14) Garcia-Beltran, W. F.; Lam, E. C.; Astudillo, M. G.; Yang, D.; Miller, T. E.; Feldman, J.; Hauser, B. M.; Caradonna, T. M.; Clayton, K. L.; Nitido, A. D.; Murali, M. R.; Alter, G.; Charles, R. C.; Dighe, A.; Branda, J. A.; Lennerz, J. K.; Lingwood, D.; Schmidt, A. G.; Iafate, A. J.; Balazs, A. B. *Cell* **2021**, *184* (2), 476–488.
- (15) Zohar, T.; Loos, C.; Fischinger, S.; Atyeo, C.; Wang, C.; Slein, M. D.; Burke, J.; Yu, J.; Feldman, J.; Hauser, B. M.; Caradonna, T.; Schmidt, A. G.; Cai, Y.; Streeck, H.; Ryan, E. T.; Barouch, D. H.; Charles, R. C.; Lauffenburger, D. A.; Alter, G. *Cell* **2020**, *183* (6), 1508–1519.
- (16) Mathew, D.; Giles, J. R.; Baxter, A. E.; Oldridge, D. A.; Greenplate, A. R.; Wu, J. E.; Alanio, C.; Kuri-Cervantes, L.; Pampena, M. B.; D'Andrea, K.; Manne, S.; Chen, Z.; Huang, Y. J.; Reilly, J. P.; Weisman, A. R.; Ittner, C. A. G.; Kuthuru, O.; Dougherty, J.; Nzingha, K.; Han, N.; Kim, J.; Pattekar, A.; Goodwin, E. C.; Anderson, E. M.; Weirick, M. E.; Gouma, S.; Arevalo, C. P.; Bolton, M. J.; Chen, F.; Lacey, S. F.; Ramage, H.; Cherry, S.; Hensley, S. E.; Apostolidis, S. A.; Huang, A. C.; Vella, L. A.; Betts, M. R.; Meyer, N. J.; Wherry, E. J.; Alam, Z.; Addison, M. M.; Byrne, K. T.; Chandra, A.; Descamps, H. C.; Kaminskiy, Y.; Hamilton, J. T.; Noll, J. H.; Omran, D. K.; Perkey, E.; Prager, E. M.; Poeschl, D.; Shah, J. B.; Shilan, J. S.; Vanderbeck, A. N. *Science* **2020**, *369* (6508), eabc8511.
- (17) Wang, Y.; Zhang, L.; Sang, L.; Ye, F.; Ruan, S.; Zhong, B.; Song, T.; Alshukairi, A. N.; Chen, R.; Zhang, Z.; Gan, M.; Zhu, A.; Huang, Y.; Luo, L.; Mok, C. K. P.; Al Gethamy, M. M.; Tan, H.; Li, Z.; Huang, X.; Li, F.; Sun, J.; Zhang, Y.; Wen, L.; Li, Y.; Chen, Z.; Zhuang, Z.; Zhuo, J.; Chen, C.; Kuang, L.; Wang, J.; Lv, H.; Jiang, Y.; Li, M.; Lin, Y.; Deng, Y.; Tang, L.; Liang, J.; Huang, J.; Perlman, S.; Zhong, N.; Zhao, J.; Malik Peiris, J.S.; Li, Y.; Zhao, J. *J. Clin. Invest.* **2020**, *130* (10), 5235.
- (18) Robbiani, D. F.; Gaebler, C.; Muecksch, F.; Lorenzi, J. C. C.; Wang, Z.; Cho, A.; Agudelo, M.; Barnes, C. O.; Gazumyan, A.; Finkin, S.; Hagglof, T.; Oliveira, T. Y.; Viant, C.; Hurley, A.; Hoffmann, H.-H.; Millard, K. G.; Kost, R. G.; Cipolla, M.; Gordon, K.; Bianchini, F.; Chen, S. T.; Ramos, V.; Patel, R.; Dizon, J.; Shmeliovich, I.; Mendoza, P.; Hartweg, H.; Nogueira, L.; Pack, M.; Horowitz, J.; Schmidt, F.; Weisblum, Y.; Michailidis, E.; Ashbrook, A. W.; Waltari, E.; Pak, J. E.; Huey-Tubman, K. E.; Koranda, N.; Hoffman, P. R.; West, A. P.; Rice, C. M.; Hatziioannou, T.; Bjorkman, P. J.; Bieniasz, P. D.; Caskey, M.; Nussenzweig, M. C. *Nature* **2020**, *584* (7821), 437–442.
- (19) Syu, G.-D.; Dunn, J.; Zhu, H. *Molecular & Cellular Proteomics* **2020**, *19* (6), 916–927.
- (20) Jiang, H.-w.; Li, Y.; Zhang, H.-n.; Wang, W.; Yang, X.; Qi, H.; Li, H.; Men, D.; Zhou, J.; Tao, S.-c. *Nat. Commun.* **2020**, *11* (1), 3581.
- (21) Lei, Q.; Yu, C. Z.; Li, Y.; Hou, H. Y.; Xu, Z. W.; Yao, Z. J.; Zhang, Y. D.; Lai, D. Y.; Ndzouboukou, J. B.; Zhang, B.; et al. *J. Adv. Res.* **2022**, *36*, 133–145.
- (22) de Assis, R. R.; Jain, A.; Nakajima, R.; Jasinskas, A.; Felgner, J.; Obiero, J. M.; Norris, P. J.; Stone, M.; Simmons, G.; Bagri, A.; et al. *Nat. Commun.* **2021**, *12* (1), 6.
- (23) Ho, T.-S.; Du, P.-X.; Su, W.-Y.; Santos, H. M.; Lin, Y.-L.; Chou, Y.-Y.; Keskin, B. B.; Pau, C. H.; Syu, G.-D. *Biosens. Bioelectron.* **2022**, *204*, 114067. Tan, C. W.; Chia, W. N.; Qin, X.; Liu, P.; Chen, M. I.; Tiu, C.; Hu, Z.; Chen, V. C.; Young, B. E.; Sia, W. R.; et al. *Nat. Biotechnol.* **2020**, *38* (9), 1073–1078.
- (24) Kiew, L. V.; Chang, C. Y.; Huang, S. Y.; Wang, P. W.; Heh, C. H.; Liu, C. T.; Cheng, C. H.; Lu, Y. X.; Chen, Y. C.; Huang, Y. X.; et al. *Biosens Bioelectron* **2021**, *183*, 113213.
- (25) Prévost, J.; Finzi, A. *Cell Host & Microbe* **2021**, *29* (3), 322–324. Hou, Y. J.; Chiba, S.; Halfmann, P.; Ehre, C.; Kuroda, M.; Dinnon, K. H.; Leist, S. R.; Schafer, A.; Nakajima, N.; Takahashi, K.; Lee, R. E.; Mascenik, T. M.; Graham, R.; Edwards, C. E.; Tse, L. V.; Okuda, K.; Markmann, A. J.; Bartelt, L.; de Silva, A.; Margolis, D. M.; Boucher, R. C.; Randell, S. H.; Suzuki, T.; Gralinski, L. E.; Kawaoka, Y.; Baric, R. S. *Science* **2020**, *370* (6523), 1464–1468. Alam, I.; Radovanovic, A.; Incitti, R.; Kamau, A. A.; Alarawi, M.; Azhar, E. I.; Gojobori, T. *Lancet Infectious Diseases* **2021**, *21* (5), 602.
- (26) Barnes, C. O.; Jette, C. A.; Abernathy, M. E.; Dam, K. A.; Esswein, S. R.; Gristick, H. B.; Malyutin, A. G.; Sharaf, N. G.; Huey-Tubman, K. E.; Lee, Y. E.; et al. *Nature* **2020**, *588* (7839), 682–687.
- (27) Gallo Marin, B.; Aghagoli, G.; Lavine, K.; Yang, L.; Siff, E. J.; Chiang, S. S.; Salazar-Mather, T. P.; Dumenco, L.; Savaria, M. C.; Aung, S. N.; et al. *Rev. Med. Virol* **2021**, *31* (1), 1–10.
- (28) Abd El-Aziz, T. M.; Al-Sabi, A.; Stockand, J. D. *Signal Transduction and Targeted Therapy* **2020**, *5*, 258. Yan, R.; Zhang, Y.; Li, Y.; Xia, L.; Guo, Y.; Zhou, Q. *Science* **2020**, *367* (6485), 1444–1448.
- (29) Cheng, L.; Zhang, X.; Chen, Y.; Wang, D.; Zhang, D.; Yan, S.; Wang, H.; Xiao, M.; Liang, T.; Li, H.; Xu, M.; Hou, X.; Dai, J.; Wu, X.; Li, M.; Lu, M.; Wu, D.; Tian, R.; Zhao, J.; Zhang, Y.; Cao, W.; Wang, J.; Yan, X.; Zhou, X.; Liu, Z.; Xu, Y.; He, F.; Li, Y.; Yu, X.; Zhang, S. *Sig. Transduct. Target. Ther.* **2021**, *6*, 304.
- (30) Chao, Y. X.; Röttschke, O.; Tan, E.-K. *Brain Behav Immun* **2020**, *87*, 182–183.